Title

Polyphenols as alternative treatments of COVID-19.

Authors

Wu, Yifei

Pegan, Scott

Crich, David

et al.

Publication Date

2021

DOI

10.1016/j.csbj.2021.09.022

Peer reviewed

Computational and Structural Biotechnology Journal 19 (2021) 5371–5380

COMPUTATIONAL AND STRUCTURAL BIOTECHNOLOGY JOURNAL

journal homepage: www.elsevier.com/locate/csbj

Polyphenols as alternative treatments of COVID-19

Yifei Wu [a], Scott D. Pegan [b], David Crich [c], Ellison Desrochers [d], Edward B. Starling [d], Madelyn C. Hansen [d], Carson Booth [d], Lauren Nicole Mullininx [d], Lei Lou [a], Kuan Y. Chang [e,*], Zhong-Ru Xie [a,*]

[a] School of Electrical and Computer Engineering, College of Engineering, University of Georgia, Athens 30602, GA, USA
[b] Division of Biomedical Sciences., School of Medicine, University of California Riverside, 92521, CA, USA
[c] Department of Pharmaceutical and Biomedical Sciences, College of Pharmacy, University of Georgia, Athens 30602, GA, USA
[d] Franklin College of Arts and Sciences, University of Georgia, Athens 30602, GA, USA
[e] Department of Computer Science and Engineering, National Taiwan Ocean University, Keelung 202, Taiwan, ROC

ARTICLE INFO

Article history:
Received 31 May 2021
Received in revised form 9 September 2021
Accepted 18 September 2021
Available online 20 September 2021

Keywords:
COVID-19
Virtual screening
Main protease
Papain-like protease
MD simulation
Natural products
Polyphenols

ABSTRACT

Although scientists around the world have put lots of effort into the development of new treatments for COVID-19 since the outbreak, no drugs except Veklury (remdesivir) have been approved by FDA. There is an urgent need to discover some alternative antiviral treatment for COVID-19. Because polyphenols have been shown to possess antiviral activities, here we conducted a large-scale virtual screening for more than 400 polyphenols. Several lead compounds such as Petunidin 3-O-(6″-p-coumaroyl-glucoside) were identified to have promising binding affinities and convincing binding mechanisms. Analyzing the docking results and ADME properties sheds light on the potential efficacy of the top-ranked drug candidates and pinpoints the key residues on the target proteins for the future of drug development.

1. Introduction

In March 2020, the World Health Organization declared a global pandemic of the novel coronavirus disease (COVID-19) [1]. This outbreak continues to wreak havoc around the world, causing over 640,000 deaths in the United States and over 4.5 million deaths worldwide by the end of August 2021 [2]. Thus, rapid discovery of small-molecule antiviral drugs that are therapeutic against COVID-19 continues to be a significant task [3].

SARS-CoV-2, the viral agent responsible for COVID-19, is an enveloped, positive-sense, single-stranded RNA virus [4,5]. Coronaviruses contain the largest-known RNA virus genomes, being roughly 26–32 kb and made up of at least six open reading frames (ORFs) encoding for proteins [5]. RNA viruses such as SARS-CoV-2 are replicated by releasing these RNA genomes into host cells, which in turn translate that RNA into proteins as if the viral RNA were the host cell's own RNA. The major ORF of SARS-CoV-2 encodes two overlapping polyproteins, PP1A and PP1B. These proteins are generated in the host cell and then cleaved into 16 non-structural proteins (NSP1-16) by two proteolytic enzymes: the main protease (M^{pro}) and papain-like protease (PL^{pro}) [6]. These NSPs then initiate replication and transcription of the viral genome by assembling the viral replicase complex on host cells membranes [3,7,8]. Thus, M^{pro} and PL^{pro} play vital roles in the replication of SARS-CoV-2 in the body; without them, the NSPs would not be released from the larger polyproteins, PP1A and PP1B.

The importance of these proteases to the viral life cycle has led researchers to wonder if they could be inactivated, and whether a protease inhibitor would be a useful treatment for COVID-19. Although coronaviruses cannot replicate if the proteolytic activity of PL^{pro} or M^{pro} is blocked [9], no PL^{pro} and M^{pro} inhibitors used for COVID-19 treatment have yet been approved. PL^{pro} not only cleaves PP1A and PP1B at three distinct sites between NSP1-4, but also helps coronaviruses to elude the host's immune response through competitive interaction with ubiquitin and ISG15 [10]. Certain inhibitors of the PL^{pro} from SARS-CoV, the virus responsible for the 2003 global outbreak of severe acute respiratory syndrome (SARS), also target the PL^{pro} from SARS-CoV-2 and exhibit antiviral activity in monkey cells *in vitro* [10]. Furthermore, PL^{pro} inhibition reduces the cytopathogenic effect and replication of SARS-CoV-2 while maintaining the interferon antiviral response *in vitro* [11]. On the other hand, M^{pro} exclusively cleaves PP1A and PP1B at 11 distinct sites immediately following a glutamine residue [6]. Because no human host cell proteases have this substrate specificity, M^{pro} is an ideal drug target [5,12,13]. A drug used to treat feline infectious peritonitis, a lethal coronavirus infection that

* Corresponding authors.
E-mail addresses: kchang@email.ntou.edu.tw (K.Y. Chang), paulxie@uga.edu (Z.-R. Xie).

https://doi.org/10.1016/j.csbj.2021.09.022
2001-0370/Published by Elsevier B.V. on behalf of Research Network of Computational and Structural Biotechnology.

affects cats, has been found to be capable of inhibiting the SARS-CoV-2 M^{pro} and blocking viral replication [14]. Two protease inhibitors approved for treating hepatitis C virus have been demonstrated to inhibit the SARS-CoV-2 M^{pro} and show strong antiviral activity in a mouse model [15]. Thus, further investigation into inhibitors of PL^{pro} and M^{pro} may very likely lead to the discovery of a safe, effective treatment for COVID-19.

Polyphenols are secondary plant metabolites with a plethora of health benefits, including strong antioxidant properties that defend against oxidative damage by free radicals and prevent chronic disease [16]. In light of the ongoing pandemic, researchers have investigated polyphenols' antiviral efficacy against COVID-19. Ghosh *et al.* found that the green tea polyphenols epigallocatechin gallate (EGCG), epicatechingallate, and gallocatechin-3-gallate interact strongly with one or both of the catalytic residues of the SARS-CoV-2 M^{pro} [17], and later demonstrated that six polyphenols from *Broussonetia papyrifera* inhibit the catalytic activity of M^{pro} as well [18]. Khan *et al.* also found that EGCG interacted strongly with M^{pro} [19]. Ansari *et al.* found that luteolin had a higher affinity for PL^{pro} than the FDA-approved antiviral drug, remdesivir [20]. However, these studies were extremely limited in scope. There are around 500 unique polyphenol structures available for download on the Phenol-Explorer 3.6 database created by Neveu *et al.* [21], and current studies investigating polyphenols as M^{pro} and PL^{pro} inhibitors are limited to a very small selection of molecules, mainly coming from green tea. Considering that promising results were found using such a small selection of polyphenols, it is possible that there are even better outcomes to be found within a larger sample.

Thus, to find potential therapeutic agents against COVID-19, this study screens a large number of polyphenols to bind to SARS-CoV-2 M^{pro} or PL^{pro}. The structures of 480 polyphenols were obtained from the aforementioned Phenol-Explorer 3.6 database, and molecular docking was conducted using Maestro. MM-GBSA scores were collected to quantify the affinity of the molecules for the proteins, and then ADME (Absorption, distribution, metabolism, and excretion) and drug-likeness properties were analyzed for further screening. Finally, several polyphenols with high affinities are identified for both proteases: Petunidin 3-O-(6″-p-coumaroyl-glucoside), Malvidin 3,5-O-diglucoside, and Cyanidin 3-O-(6″-p-coumaroyl-glucoside) bind to M^{pro} (−101.21 kcal/mol, −95.07 kcal/mol, and −90.17 kcal/mol, respectively), while Kaempferol 3-O-sophoroside 7-O-glucoside, Cyanidin 3-O-sambubioside 5-O-glucoside, and Malvidin 3-O-(6″-p-coumaroyl-glucoside) are the top polyphenols bound to PL^{pro} (−87.97 kcal/mol, −87.33 kcal/mol, and −85.70 kcal/mol, respectively). This study identifies multiple polyphenols with extremely high binding affinities to the SARS-CoV-2 M^{pro} and PL^{pro} as potential natural products used for COVID-19 treatment.

2. Materials and methods

2.1. Ligand preparation

The 3D structures of 480 tested polyphenols were retrieved from Phenol-Explorer 3.6 (http://phenol-explorer.eu/). All the polyphenolic compounds were prepared using Ligprep in Maestro 12.4 (Schrödinger). The force field was OPLS3e by default [22]. The process of preparation includes adding hydrogens, computing correct partial charges, and generating possible conformations.

2.2. Protein preparation

The protein structures of M^{pro} (PDB ID: 7BRP) and PL^{pro} (PDB ID: 6W9C) from RCSB's Protein Data Bank (https://www.rcsb.org/) [23] were prepared for use by Maestro in three steps: preprocessing, optimization, and minimization. The preprocessing included assigning bond orders, adding hydrogens, creating zero-order bonds to metals, creating disulfide, filling in missing side chains using Prime, deleting water molecules beyond 5.00 Å from het groups and generating het states using Epik [24]. PROPKA's default setting (pH = 7.0) and the OPLS3e force field were applied in optimization and minimization.

2.3. Ligand-protein docking

To estimate the interactions between target proteins and polyphenols, we conducted ligand–protein docking by using the Ligand Docking panel in Maestro. Before running docking jobs, a receptor grid box was generated based on existing ligands in protein structures. For the structure of M^{pro} (PDB ID: 7BRP), the existing ligand boceprevir was used to generate a receptor grid. In the structure of PL^{pro} (PDB ID: 6W9C), the receptor grid was generated according to the same site on SARS-CoV PL^{pro} (PDB ID: 3E9S). The size of the receptor grid box was set as default (20 Å). Ligand-protein docking was performed in extra-precision (XP) mode.

2.4. MM-GBSA calculation

To predict the binding energies of polyphenols bound to M^{pro} or PL^{pro}, we performed Prime MM-GBSA (molecular mechanics generalized Born surface area) in Maestro. In the MM-GBSA panel, the pose viewer files of the docked complex were uploaded into the MM-GBSA panel. The force field was OPLS3e.

Table 1
The results of the top 3 polyphenols bound to $M^{pro.}$

Compound	Estimated binding energy (kcal/mol)	QPlogS[a]	RO5[b]	RO3[c]	Predicted IC_{50} (nM)
Petunidin 3-O-(6″-p-coumaroyl-glucoside)	−101.21	−4.479	3	2	44.47
Malvidin 3,5-O-diglucoside	−95.07	−2.335	3	2	45.73
Cyanidin 3-O-(6″-p-coumaroyl-glucoside)	−90.17	−2.303	3	2	43.00
*Saquinavir	−93.58	−2.164	3	2	52.48
**Epigallocatechin gallate (EGCG)	−65.04	−3.554	2	2	60.73
***Papyriflavonol A	−58.38	−6.287	0	2	76.96
****Boceprevir	−72.56	−4.372	1	0	46.72

*The best-scored potential drug identified by our previous study [36]
**The best-scored potential drug identified by a previous study [17]
***The best-scored potential drug identified by a previous study [18]
**** The original ligand of 7BRP [37]
a. QPlogS is predicted aqueous solubility. The recommended range is −6.5 ∼ 0.5.
b. RO5: number of violations of Lipinski's rule of five [38]. The recommended range: maximum is 4.
c. RO3: Number of violations of Jorgensen's rule of three [39]. The recommended range: maximum is 3.

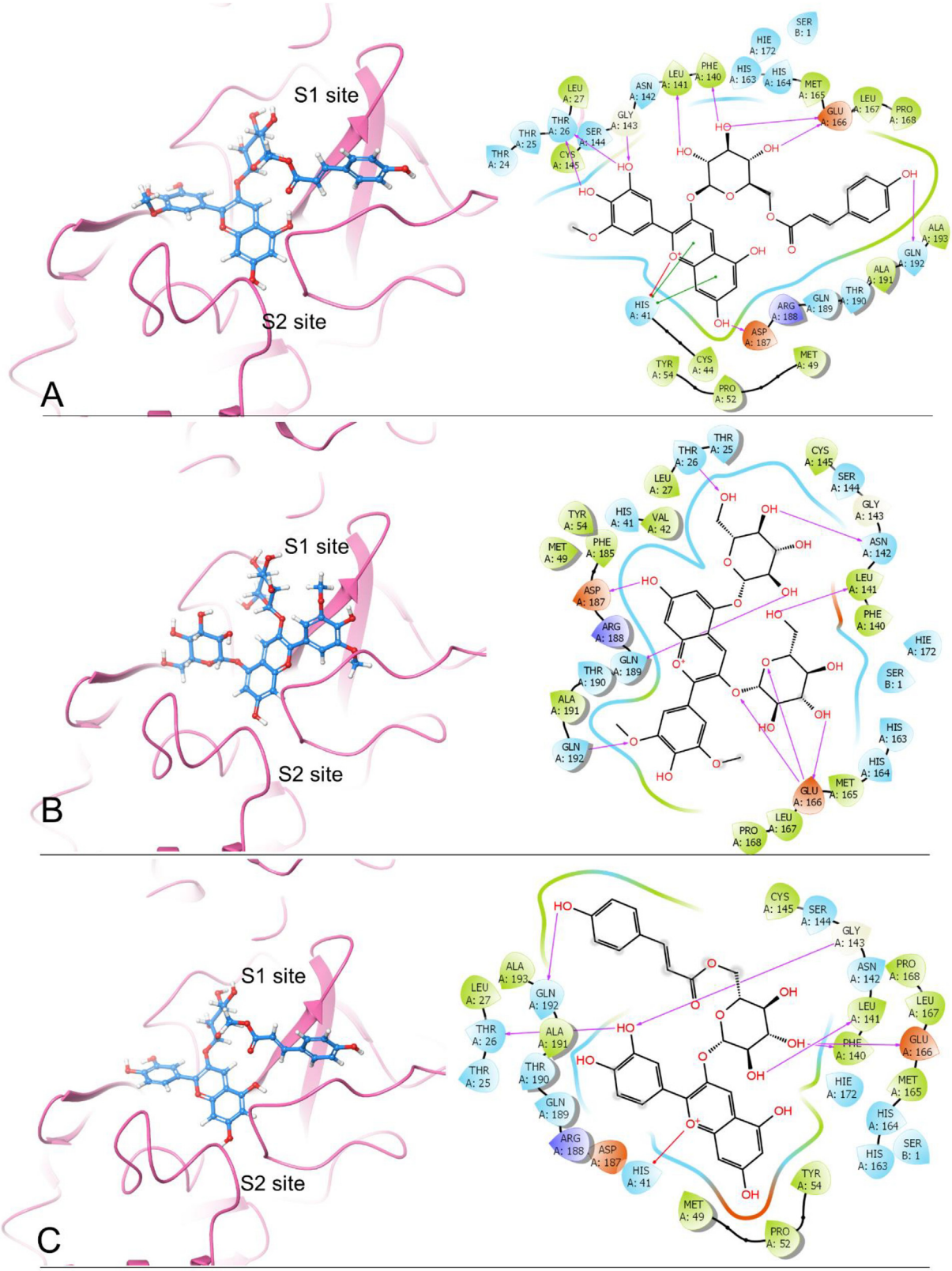

Fig. 1. The docking poses and 2-D ligand–protein interaction diagrams of 7BRP and the top three ligands: A, Petunidin 3-O-(6″-p-coumaroyl-glucoside); B, Malvidin 3,5-O-diglucoside; C, Cyanidin 3-O-(6″-p-coumaroyl-glucoside). For the docking poses, S1/S2 subsites are being shown. The purple arrow indicates the hydrogen bond; the green line represents π-π stacking; the red line represents π -cation interaction. (For interpretation of the references to colour in this figure legend, the reader is referred to the web version of this article.)

Table 2
The number of hydrogen bonds formed between the top three polyphenols and essential residues of SARS-CoV-2 M^{pro}.

	Petunidin 3-O-(6″-p-coumaroyl-glucoside)	Malvidin 3,5-O-diglucoside	Cyanidin 3-O-(6″-p-coumaroyl-glucoside)
Thr26	2	1	1
Phe140	1		1
Leu141	1	1	1
Asn142		1	
Gly143	1		1
Glu166	2	3	1
Asp187	1	1	
Gln189		1	
Gln192	1	1	1

2.5. ADME and drug-likeness properties prediction

After binding energies calculation, we applied Qikprop module in Maestro to predict ADME and drug-likeness properties for further screening [25]. For Qikprop, the top-ranked polyphenols were prepared by using Ligprep. Finally, the descriptors such as RuleOfFive (RO5) and RuleOfThree (RO3) were applied to analyze the candidates.

2.6. AutoQSAR analysis

AutoQSAR module of Schrodinger is a machine learning tool to build and apply quantitative structure–activity relationship (QSAR) models [26]. To build machine learning models, 61 M^{pro} inhibitors and 20 PLpro inhibitors were retrieved from BindingDB [27]. The best model of each protease was used to predict half-maximal inhibitory concentration (IC_{50}) of the top-ranked polyphenols. The details of the polyphenols along with their predicted IC_{50} values are presented in Tables 1 and 3.

2.7. Molecular dynamics simulation

To further investigate the dynamic interactions between target proteins (M^{pro} and PL^{pro}) and the top two polyphenols, we conducted Molecular dynamics (MD) simulations by using GROMACS version 2018.1 and CHARMM36 force field [28]. The starting coordinates of the protein–ligand complex were obtained from a ligand–protein docking study. Then, we used CHARMM-GUI to build the MD simulation solution boxes which were cubic boxes with length of 109 Å for 6W9C and 104 Å for 7BRP, and were filled with water [29–31]. Next, the minimized structures were equilibrated using an NVT ensemble (constant Number of particles, Volume, and Temperature) and NPT ensemble (the Number of particles, Pressure, and Temperature). The target equilibration temperature was 300 K. Finally, MD simulations were performed for 100 ns. After the MD simulations, we calculated the root-mean-square deviation (RMSD) and the energies.

3. Results

3.1. Docking analysis of polyphenols against SARS-CoV-2 M^{pro}

To seek effective inhibitors from polyphenols against SARS-CoV-2 M^{pro}, 480 polyphenols (ligand) were docked onto SARS-CoV-2 M^{pro} (protein: PDB ID: 7BRP). Based on the docking poses, binding energies between the protein and ligand were calculated by MM-GBSA. Compared to three top drug candidates proposed by previous studies [17,18], in Table 1, the best three protein–ligand complexes, 7BRP- Petunidin 3-O-(6″-p-coumaroyl-glucoside) (−101.21 kcal/mol), 7BRP-Malvidin 3,5-O-diglucoside (−95.07 kcal/mol), and 7BRP- Cyanidin 3-O-(6″-p-coumaroyl-glucoside) (−90.17 kcal/mol) all have better estimated binding affinities. These top three polyphenols are members of anthocyanins, which can be found in black raspberry [32]. Meanwhile, we selected four ligands: saquinavir (−93.58 kcal/mol), EGCG (−65.04 kcal/mol), papyriflavonol A (−58.38 kcal/mol), and boceprevir (−72.56 kcal/mol) as a control group. From Table 1, we find that the binding energy of Saquinavir is slightly better than that of Cyanidin 3-O-(6″-p-coumaroyl-glucoside) (−90.17 kcal/mol), however, the binding energies of Petunidin 3-O-(6″-p-coumaroyl-glucoside) and Malvidin 3,5-O-diglucosideare are better than those of the control group, which suggests the potential inhibitory effects of these polyphenols against SARS-CoV-2 M^{pro}.

By comparing the 2D ligand–protein interactions of the top three polyphenols with M^{pro} (Fig. 1), we find that they all interact with Glu166 by forming hydrogen bonds: two hydrogen bonds for Petunidin 3-O-(6″-p-coumaroyl-glucoside), three for Malvidin 3,5-O-diglucoside, and one for cyanidin 3-O-(6″-p-coumaroyl-glucoside) (Table 2). This result suggests that Glu166 is an essential residue in the binding pocket. According to the previous studies, Glu166 plays an important role in connecting the substrate binding site with the dimer interface [33], and it also forms critical interactions with the residues of N-terminal finger on the heterologous monomer [33,34]. In addition, the equivalent Glu169 on the M^{pro} of MERS-CoV is also a key residue, which is crucial in both dimerization and catalysis [35].

Furthermore, these top three polyphenols all interact with Thr26, Leu141, and Gln192 by forming hydrogen bonds. Petunidin 3-O-(6″-p-coumaroyl-glucoside) and Cyanidin 3-O-(6″-p-coumaroyl-glucoside) interact with Phe140 and Gly143 by forming hydrogen bonds. Petunidin 3-O-(6″-p-coumaroyl-glucoside) and Malvidin 3,5-O-diglucoside both interact with Asp187 by forming

Table 3
The results of the top 3 polyphenols bound to PL^{pro}.

Compound	Estimated binding energy (kcal/mol)	QPlogS[a]	RO5[b]	RO3[c]	Predicted IC_{50} (nM)
Kaempferol 3-O-sophoroside 7-O-glucoside	−87.97	−1.440	3	2	253.25
Cyanidin 3-O-sambubioside 5-O-glucoside	−87.33	−1.618	3	2	253.25
Malvidin 3-O-(6″-p-coumaroyl-glucoside)	−85.70	−4.664	3	2	243.37
*GRL-0617	−60.75	−4.952	0	0	483.16
**Luteolin	−43.53	−3.067	0	0	253.25
***VIR251	−64.40	−0.066	2	2	261.62

*a known prodrug of PL^{pro} identified in our previous study [10].
**the best-scored potential drug identified by the previous study [20].
*** a peptide inhibitor in the structure of 6WX4 [75].
a. QPlogS is predicted aqueous solubility. The recommended range is $-6.5 \sim 0.5$.
b. RO5: number of violations of Lipinski's rule of five [38]. The recommended range: maximum is 4.
c. RO3: Number of violations of Jorgensen's rule of three [39]. The recommended range: maximum is 3.

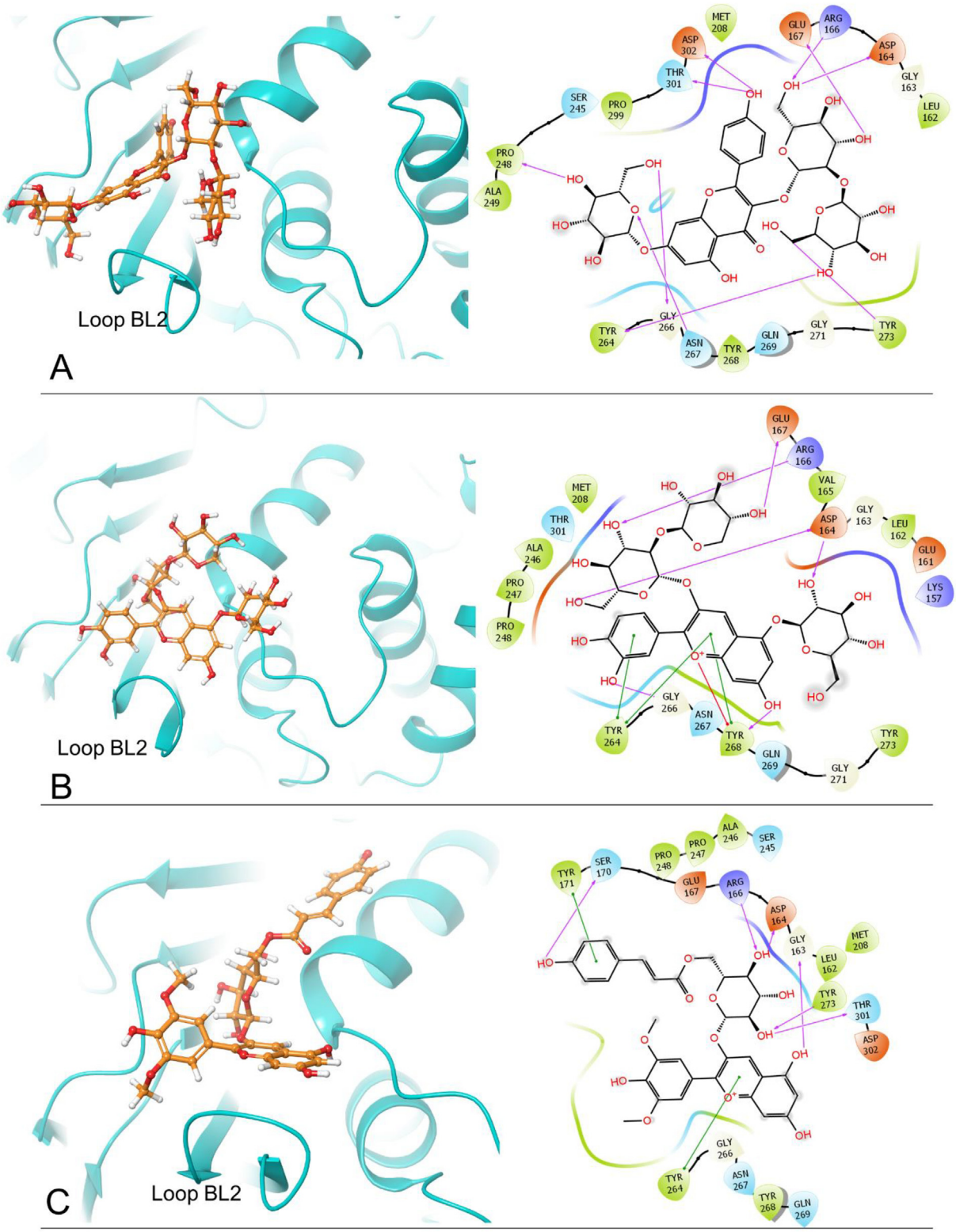

Fig. 2. The docking poses and 2-D ligand–protein interaction diagrams of 6W9C and the top three ligands: A, Kaempferol 3-O-sophoroside 7-O-glucoside; B, Cyanidin 3-O-sambubioside 5-O-glucoside; C, Malvidin 3-O-(6″-p-coumaroyl-glucoside). The pink arrow indicates the hydrogen bond; the green line represents π-π stacking; the red line represents π-cation interaction. (For interpretation of the references to colour in this figure legend, the reader is referred to the web version of this article.)

one hydrogen bond each. Additionally, His41 is also a critical residue which can interact with the top three polyphenols. Petunidin 3-O-(6″-p-coumaroyl-glucoside) interacts with His41 by forming two π-π stackings and one π-cation interaction, and Cyanidin 3-O-(6″-p-coumaroyl-glucoside) interacts with His41 via one π-cation interaction. The number of hydrogen bonds between the

Table 4
The number of hydrogen bonds formed between the top three polyphenols and essential residues of SARS-CoV-2 PL^{pro}.

	Kaempferol 3-O-sophoroside 7-O-glucoside	Cyanidin 3-O-sambubioside 5-O-glucoside	Malvidin 3-O-(6″-p-coumaroyl-glucoside)
Gly163			1
Asp164	1	2	1
Arg166	1	1	1
Glu167	1	1	
Ser170			1
Pro248	1		
Tyr264	1		
Gly266	1	1	
Asn267	1		
Tyr268		1	
Tyr273	1		1
Thr301	1		1
Asp302	1		

top three polyphenols and essential residues are listed in Table 1. Accordingly, we propose that Petunidin 3-O-(6″-p-coumaroyl-glucoside), Malvidin 3,5-O-diglucoside, and Cyanidin 3-O-(6″-p-coumaroyl-glucoside) are the three best drug candidates among all 480 polyphenols tested against SARS-CoV-2 M^{pro}.

To further screen the drug candidates for M^{pro}, we calculated drug-likeness properties and predicted IC_{50} on the top three polyphenols by using Qikprop and AutoQSAR, respectively. The results are shown in Table 1. The polyphenols whose Qikprop descriptors (QPlogS, RuleOfFive, and RuleOfThree) fell out of the recommended range were excluded. For the results of AutoQSAR, it is interesting to note that the predicted IC_{50} values of the top three polyphenols are all lower than 50 nM and Cyanidin 3-O-(6″-p-coumaroyl-glucoside) shows the best predicted IC_{50}, which is generally consistent with the docking results.

3.2. Docking analysis of polyphenols against SARS-CoV-2 PL^{pro}

To identify the best inhibitors of SARS-CoV-2 PL^{pro}, we also docked 480 polyphenols on SARS-CoV-2 PL^{pro} (PDB ID: 6W9C) by performing ligand–protein docking and MM-GBSA calculations (see Table 3). Consequently, the three best compounds with the top MM-GBSA binding energies were Kaempferol 3-O-sophoroside 7-O-glucoside (−87.97 kcal/mol), Cyanidin 3-O-sambubioside 5-O-glucoside (−87.33 kcal/mol), and Malvidin 3-O-(6″-p-coumaroyl-glucoside) (−85.70 kcal/mol). Kaempferol 3-O-sophoroside 7-O-glucoside belongs to the group of flavonols. Cyanidin 3-O-sambubioside 5-O-glucoside and Malvidin 3-O-(6″-p-coumaroyl-glucoside) belong to the group of anthocyanins. Meanwhile, a known PL^{pro} inhibitor GRL-0617 [10], the best-scored potential drug luteolin [20], and a peptide inhibitor in the structure 6WX4 were selected as control. From Table 3, we find that the top three polyphenols show better binding energies than the control compounds, which indicates that these polyphenols might have stronger inhibitory effects.

From the 2D ligand–protein interactions in Fig. 2, we find that the top three compounds all can interact with Asp164 and Arg166 by forming hydrogen bonds. Kaempferol 3-O-sophoroside 7-O-glucoside and Malvidin 3-O-(6″-p-coumaroyl-glucoside) interact with Asp164 by forming one hydrogen bond, respectively. Cyanidin 3-O-sambubioside 5-O-glucoside interacts with Asp164 by forming two hydrogen bonds. These three compounds form one hydrogen bond with Arg166, respectively. Moreover, Kaempferol 3-O-sophoroside 7-O-glucoside can interact with Gly266 and Asn267 by forming one hydrogen bond, respectively. Cyanidin 3-O-sambubioside 5-O-glucoside interacts with Gly266 and Tyr268 by forming one hydrogen bond, respectively. Notably, Gly266, Asn267, and Tyr268 are residues on blocking loop 2 (BL2), and BL2 plays an important role in inhibitor binding [40]. Hence, the interactions between the top two polyphenols and BL2 suggest strong inhibitory effects. Accordingly, we conclude that these two polyphenols can tightly bind onto the binding pocket. The number of hydrogen bonds between these three compounds and the essential residues are listed in Table 4.

3.3. Molecular dynamics (MD) simulation

To further analyze the stability of complexes, we conducted MD simulation to calculate RMSD and energy for the top two candi-

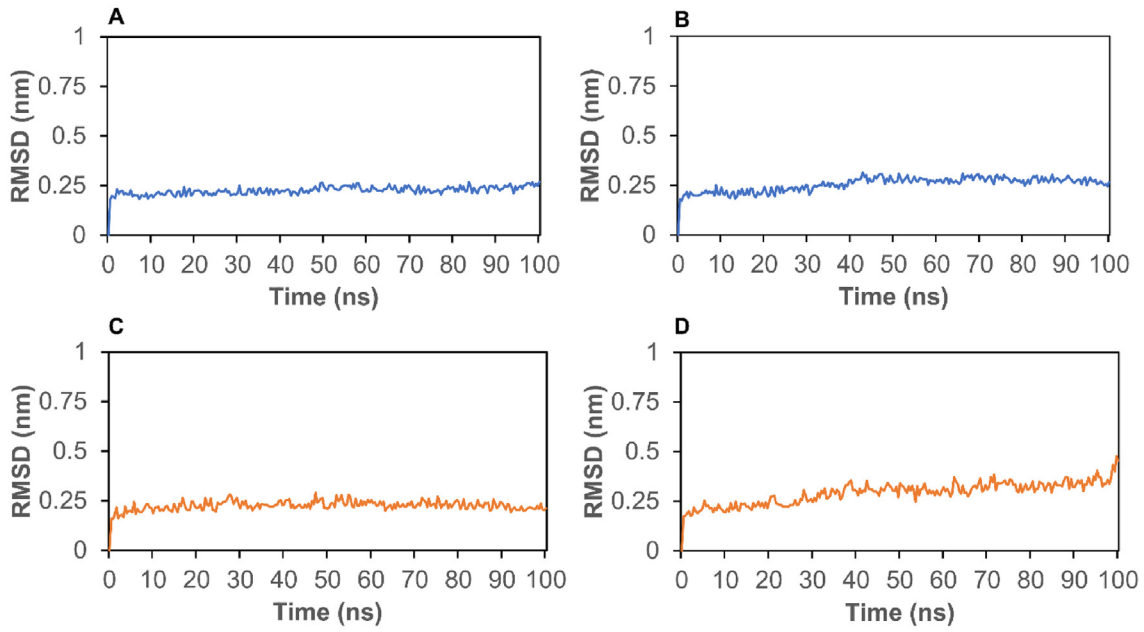

Fig. 3. The RMSD of protein–ligand complexes. A, 7BRP- Petunidin 3-O-(6″-p-coumaroyl-glucoside); B, 7BRP- Malvidin 3,5-O-diglucoside; C, 6W9C- Kaempferol 3-O-sophoroside 7-O-glucoside; D, 6W9C- Cyanidin 3-O-sambubioside 5-O-glucoside.

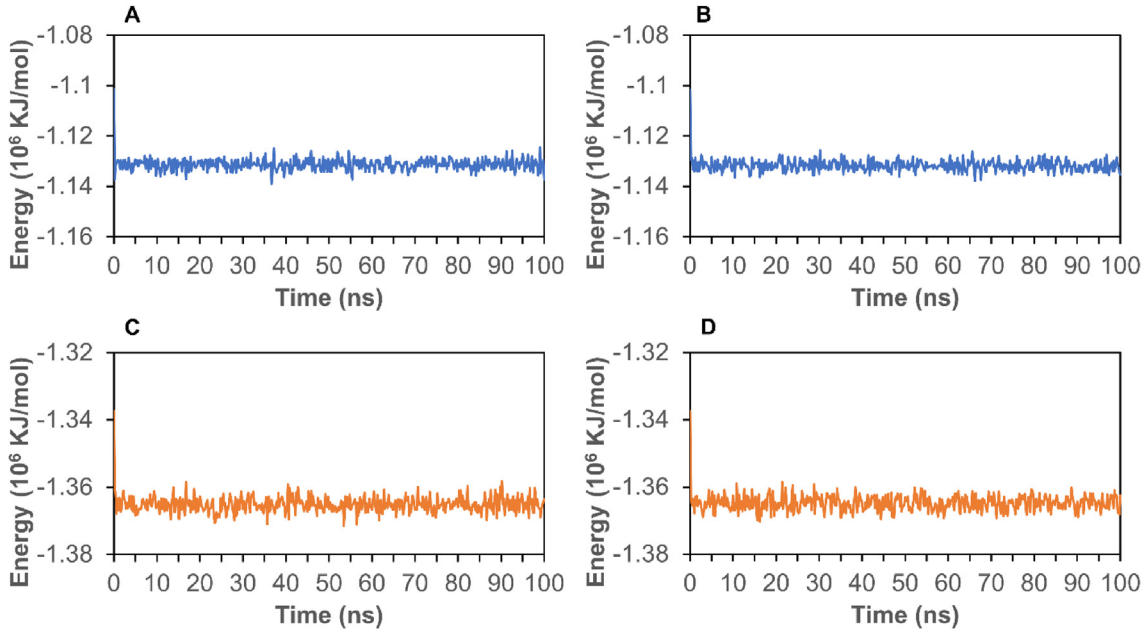

Fig. 4. The energy of protein–ligand complexes. A, 7BRP- Petunidin 3-O-(6″-p-coumaroyl-glucoside); B, 7BRP- Malvidin 3,5-O-diglucoside; C, 6W9C- Kaempferol 3-O-sophoroside 7-O-glucoside; D, 6W9C- Cyanidin 3-O-sambubioside 5-O-glucoside.

dates. First, RMSD can be used to assess the stability of a protein–ligand complex. As shown in Fig. 3A, the RMSD for the complex of 7BRP- Petunidin 3-O-(6″-p-coumaroyl-glucoside) stabilized around 0.25 nm between 5 ns and 100 ns. In Fig. 3B, the RMSD of 7BRP-Malvidin 3,5-O-diglucoside stabilized at 0.25 nm from 10 ns to 40 ns, and then stabilized around 0.3 nm after 40 ns. The RMSD of 6W9C with Kaempferol 3-O-sophoroside 7-O-glucoside stabilized at 0.25 nm from 4 to 100 ns (Fig. 3C). From Fig. 3D, we find that the RMSD of 6W9C with Cyanidin 3-O-sambubioside 5-O-glucoside stabilized at 0.25 nm before 30 ns, and then stabilized around 0.35 nm from 30 to 90 ns. Moreover, the total energies of these four complexes are shown in Fig. 4. The energies of 7BRP complexes stabilized at around -1.13×10^6 KJ/mol (Fig. 4A and B). Interestingly, the energy of 6W9C complexes stabilized at around -1.365×10^6 KJ/mol (Fig. 4C and D). The RMSD and energy analysis show that the complexes of M^{pro} or PL^{pro} with their respective top two polyphenols stay stable during the simulation process.

4. Discussion

Many studies have shown natural products possessing antiviral properties against the Epstein-Barr virus [41,42], herpes simplex virus [43,44], influenza virus [45], and other viruses targeting the respiratory tract [45,46–50,74]. Since the 2003 outbreak of SARS, a number of natural products have been reported to inhibit the coronavirus which causes SARS (SARS-CoV) or its target proteins [49–64]. In addition, previous studies demonstrate that many polyphenols, including quercetin and its glycosylated derivatives, inhibit cell proliferation of tumor cells or microorganisms [65–68]. Glycosylation of polyphenols could enhance water solubility, bioavailability, and their binding affinities to significant enzymes and improve the drug efficacy [69–71]. This result not only suggests that polyphenols are potential drug candidates, but also indicates that this study discovered more polyphenols for COVID-19 treatment.

Based on the docking pose of each target protein, we find that the key residue(s) can interact with the best inhibitor candidate via multiple interactions. First, in the structure of M^{pro}, Glu166 is a key residue for M^{pro} dimerization and substrate binding pocket creation [72]. The best inhibitor candidate Petunidin 3-O-(6″-p-coumaroyl-glucoside) interacts with Glu166 side chain by forming two hydrogen bonds (Fig. 5A), which makes an impact on increasing the binding energy. This result is consistent with the finding in our previous research which showed that saquinvir interacts with Glu166 [36]. Accordingly, Glu166 is a key residue for M^{pro} inhibitor discovery. In the structure of PL^{pro}, the residues (Gly266-Gly271) in the BL2 loop are critical for inhibitor binding [7,73]. From Fig. 5B, we find that the best candidate of PL^{pro} Kaempferol 3-O-sophoroside 7-O-glucoside forms hydrogen bonds with Gly266 and Asn267 which are the residues in the BL2 loop. Additionally, the second-best candidate Cyanidin 3-O-sambubioside 5-O-glucoside form one hydrogen bond with Tyr268 which is also an important residue in the BL2 loop. Therefore, more interactions between the inhibitor and the BL2 loop may increase the binding affinity.

In summary, this study demonstrates the potential of polyphenols being an alternative treatment of COVID-19. The docking results agree with previous studies identifying the key residues interacting with the binding inhibitors or prodrugs, but the proposed inhibitors in this study possess even better estimated binding affinities. However, most of the top-ranked polyphenols cannot be ordered for validation experiments currently. We are attempting to obtain some of them from other labs or produce them ourselves. The much better estimated binding affinities than previously identified compounds and rational binding mechanisms support their potential efficacy and provide the clues for the future drug development.

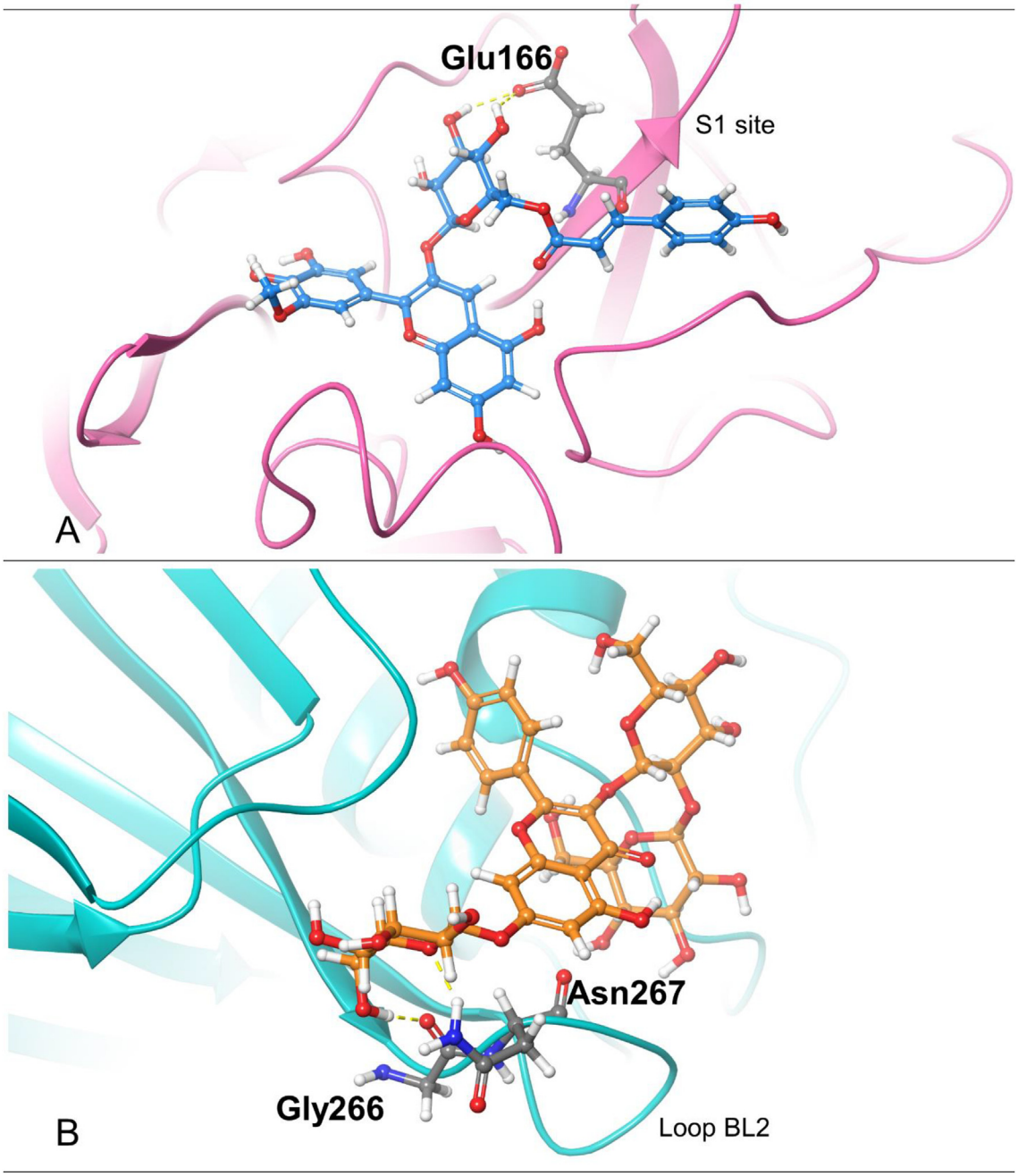

Fig. 5. 3D interaction diagrams showing the interactions between the best ligand and the key residue(s). A, Petunidin 3-O-(6″-p-coumaroyl-glucoside) interacts with the side chain of Glu166 via hydrogen bonds (yellow dash lines) on M^{pro} (PDB ID: 7BRP); B, Kaempferol 3-O-sophoroside 7-O-glucoside interacts with Gly266 and Asn267 via hydrogen bonds (yellow dash lines) on PL^{pro} (PDB ID: 6W9C). (For interpretation of the references to colour in this figure legend, the reader is referred to the web version of this article.)

Declaration of Competing Interest

The authors declare that they have no known competing financial interests or personal relationships that could have appeared to influence the work reported in this paper.

Acknowledgments

In this research, YW, LL, and ZRX were supported by a faculty seed grant from the office of research, University of Georgia and KYC was supported by Ministry of Science and Technology, R.O.C. under MOST-108-2221-E-019-052. We would like to acknowledgment Georgia Advanced Computing Resource Center (GACRC) and the College of Engineering's IT department of the UGA for technical support. This work used the Extreme Science and Engineering Discovery Environment (XSEDE) Bridges GPU at the Pittsburgh Supercomputing Center through allocation TGDPP180005.

Appendix A. Supplementary data

Supplementary data to this article can be found online at https://doi.org/10.1016/j.csbj.2021.09.022.

References

[1] Cucinotta D, Vanelli M. WHO Declares COVID-19 a Pandemic. Acta Biomed 2020;91:157–60. https://doi.org/10.23750/abm.v91i1.9397.

[2] Dong E, Du H, Gardner L. An interactive web-based dashboard to track COVID-19 in real time. Lancet Infect Dis. 2020;20:533–4. https://doi.org/10.1016/S1473-3099(20)30120-1.

[3] Klemm T, Ebert G, Calleja DJ, Allison CC, Richardson LW, Bernardini JP, et al. Mechanism and inhibition of the papain-like protease, PLpro, of SARS-CoV-2. EMBO J 2020;39:1–17.

[4] V'kovski P, Kratzel A, Steiner S, Stalder H, Thiel V. Coronavirus biology and replication: implications for SARS-CoV-2. Nat Rev Microbiol 2021;19:155–70. https://doi.org/10.1038/s41579-020-00468-6.

[5] Ullrich S, Nitsche C. The SARS-CoV-2 main protease as drug target. Bioorganic Med Chem Lett 2020;30:. https://doi.org/10.1016/j.bmcl.2020.127377127377.

[6] Wu J, Yuan X, Wang B, Gu R, Li W, Xiang X, et al. Severe acute respiratory syndrome coronavirus 2: from gene structure to pathogenic mechanisms and potential therapy. Front Microbiol 2020;11:1576. https://doi.org/10.3389/fmicb.2020.01576.

[7] Báez-Santos YM, St. John SE, Mesecar AD. The SARS-coronavirus papain-like protease: structure, function and inhibition by designed antiviral compounds. Antiviral Res 2015;115:21–38. https://doi.org/10.1016/j.antiviral.2014.12.015.

[8] Barretto N, Jukneliene D, Ratia K, Chen Z, Mesecar AD, Baker SC. The papain-like protease of severe acute respiratory syndrome coronavirus has deubiquitinating activity. J Virol 2005;79:15189–98.

[9] Kim JC, Spence RA, Currier PF, Lu X, Denison MR. Coronavirus protein processing and RNA synthesis is inhibited by the cysteine proteinase inhibitor E64d. Virology 1995;208:1–8.

[10] Freitas BT, Durie IA, Murray J, Longo JE, Miller HC, Crich D, et al. Characterization and noncovalent inhibition of the deubiquitinase and deISGylase activity of SARS-CoV-2 papain-like protease. ACS Infect Dis 2020;6:2099–109. https://doi.org/10.1021/acsinfecdis.0c00168.

[11] Shin D, Mukherjee R, Grewe D, Bojkova D, Baek K, Bhattacharya A, et al. Papain-like protease regulates SARS-CoV-2 viral spread and innate immunity. Nature 2020;587:657. https://doi.org/10.1038/s41586-020-2601-5.

[12] Baby K, Maity S, Mehta CH, Suresh A, Nayak UY, Nayak Y. Targeting SARS-CoV-2 main protease: a computational drug repurposing study. Arch Med Res 2021;52:38–47. https://doi.org/10.1016/j.arcmed.2020.09.013.

[13] Zhang L, Lin D, Sun X, Curth U, Drosten C, Sauerhering L, et al. Crystal structure of SARS-CoV-2 main protease provides a basis for design of improved a-ketoamide inhibitors. Science (80-) 2020;368:409–12. https://doi.org/10.1126/science.abb3405.

[14] Vuong W, Khan MB, Fischer C, Arutyunova E, Lamer T, Shields J, et al. Feline coronavirus drug inhibits the main protease of SARS-CoV-2 and blocks virus replication. Nat Commun 2020;11. https://doi.org/10.1038/s41467-020-18096-2.

[15] Qiao J, Li Y-S, Zeng R, Liu F-L, Luo R-H, Huang C, et al. SARS-CoV-2 M pro inhibitors with antiviral activity in a transgenic mouse model. Science (80-) 2021;371:1374–8. https://doi.org/10.1126/science.abf1611.

[16] Pandey KB, Rizvi SI. Plant polyphenols as dietary antioxidants in human health and disease. 2009. https://doi.org/10.1016/B978-0-12-849873-6.00001-7%0Ahttp://saber.ucv.ve/ojs/index.php/rev_venes/article/view/1112%0Ahttps://www.bps.go.id/dynamictable/2018/05/18/1337/persentase-panjang-jalan-tol-yang-beroperasi-menurut-operatornya-2014.html.

[17] Ghosh R, Chakraborty A, Biswas A, Chowdhuri S. Evaluation of green tea polyphenols as novel corona virus (SARS CoV-2) main protease (Mpro) inhibitors–an in silico docking and molecular dynamics simulation study. J Biomol Struct Dyn 2020:1–13. https://doi.org/10.1080/07391102.2020.1779818.

[18] Ghosh R, Chakraborty A, Biswas A, Chowdhuri S. Identification of polyphenols from Broussonetia papyrifera as SARS CoV-2 main protease inhibitors using in silico docking and molecular dynamics simulation approaches. J Biomol Struct Dyn 2020. https://doi.org/10.1080/07391102.2020.1802347.

[19] Khan MF, Khan MA, Khan ZA, Ahamad T, Ansari WA. Identification of dietary molecules as therapeutic agents to combat COVID-19 using molecular docking studies. Res Sq 2020:1–17.

[20] Ansari WA, Ahamad T, Khan MA, Khan ZA, Luteolin Khan MF. A dietary molecule as potential anti-COVID-19 agent. Res Sq 2020:1–10.

[21] Neveu V, Perez-Jiménez J, Vos F, Crespy V, du Chaffaut L, Mennen L, et al. Phenol-explorer: an online comprehensive database on polyphenol contents in foods. Database (Oxford) 2010;2010. https://doi.org/10.1093/database/bap024.

[22] Harder E, Damm W, Maple J, Wu C, Reboul M, Xiang JY, et al. OPLS3: a force field providing broad coverage of drug-like small molecules and proteins. J Chem Theory Comput 2016;12:281–96.

[23] Berman HM, Westbrook J, Feng Z, Gilliland G, Bhat TN, Weissig H, et al. The protein data bank. Nucleic Acids Res 2000;28:235–42. , http://www.ncbi.nlm.nih.gov/pubmed/10592235.

[24] Shelley JC, Anuradha AE, Ae C, Ae LLF, Greenwood JR, Mathew AE, et al. Epik: a software program for pK a prediction and protonation state generation for drug-like molecules. J Comput Aided Mol Des 2007;21:681–91.

[25] Schrödinger Release 2021-3: QikProp, Schrödinger, LLC, New York, NY, 2021.

[26] Dixon SL, Duan J, Smith E, Von Bargen CD, Sherman W, Repasky MP. AutoQSAR: an automated machine learning tool for best-practice quantitative structure-activity relationship modeling. Future Med Chem 2016;8:1825–39.

[27] Liu T, Lin Y, Wen X, Jorissen RN, Gilson MK. BindingDB: a web-accessible database of experimentally determined protein-ligand binding affinities. Nucleic Acids Res 2007;35. https://doi.org/10.1093/nar/gkl999.

[28] Vanommeslaeghe K, Hatcher E, Acharya C, et al. CHARMM general force field: a force field for drug-like molecules compatible with the CHARMM all-atom additive biological force fields. J Comput Chem 2010;31:671–90.

[29] Lee J, Cheng X, Swails JM, Yeom MS, Eastman PK, Lemkul JA, et al. CHARMM-GUI input generator for NAMD, GROMACS, AMBER, OpenMM, and CHARMM/OpenMM simulations using the CHARMM36 additive force field. J Chem Theory Comput 2016;12:405–13.

[30] Jo S, Kim T, Iyer VG, Im W. CHARMM-GUI: a web-based graphical user interface for CHARMM. J Comput Chem 2008;29:1859–65.

[31] Brooks BR, Brooks CL, Mackerell AD, Nilsson L, Petrella RJ, Roux B, et al. CHARMM: the biomolecular simulation program. J Comput Chem 2009;30:1545–614.

[32] Artemio Z, Tulio J, Reese RN, Wyzgoski FJ, Rinaldi PL, Fu R, et al. Cyanidin 3-rutinoside and cyanidin 3-xylosylrutinoside as primary phenolic antioxidants in black raspberry. J Agric Food Chem 2008;56:1880–8.

[33] Cheng SC, Chang GG, Chou CY. Mutation of glu-166 blocks the substrate-induced dimerization of SARS coronavirus main protease. Biophys J 2010;98:1327–36. https://doi.org/10.1016/j.bpj.2009.12.4272.

[34] Hsu MF, Kuo CJ, Chang KT, Chang HC, Chou CC, Ko TP, et al. Mechanism of the maturation process of SARS-CoV 3CL protease. J Biol Chem 2005;280:31257–66. https://doi.org/10.1074/jbc.M502577200.

[35] Ho BL, Cheng SC, Shi L, Wang TY, Ho KI, Chou CY. Critical assessment of the important residues involved in the dimerization and catalysis of MERS Coronavirus Main Protease. PLoS ONE 2015;10:1–18.

[36] Wu Y, Chang KY, Lou L, Edwards LG, Doma BK, Xie ZR. In silico identification of drug candidates against COVID-19. Informatics Med Unlocked 2020;21:. https://doi.org/10.1016/j.imu.2020.100461100461.

[37] Fu L, Ye F, Feng Y, Yu F, Wang Q, Wu Y, et al. Both Boceprevir and GC376 efficaciously inhibit SARS-CoV-2 by targeting its main protease. Nat Commun 2020;11.

[38] Lipinski CA, Lombardo F, Dominy BW, Feeney PJ. Experimental and computational approaches to estimate solubility and permeability in drug discovery and development settings. Adv Drug Deliv Rev 2001;46:3–26.

[39] Jorgensen WL, Duffy EM. Prediction of drug solubility from structure. Adv Drug Deliv Rev 2002;54:355–66.

[40] Lee H, Lei H, Santarsiero BD, Gatuz JL, Cao S, Rice AJ, et al. Inhibitor recognition specificity of MERS-CoV papain-like protease may differ from that of SARS-CoV. ACS Chem Biol 2015;10:1456–65.

[41] De Leo A, Arena G, Lacanna E, Oliviero G, Colavita F, Mattia E. Resveratrol inhibits Epstein Barr Virus lytic cycle in Burkitt's lymphoma cells by affecting multiple molecular targets. Antiviral Res 2012;96:196–202. https://doi.org/10.1016/j.antiviral.2012.09.003.

[42] Yiu C-Y, Chen S-Y, Chang L-K, Chiu Y-F, Lin T-P. Inhibitory effects of resveratrol on the Epstein-Barr virus lytic cycle. Molecules 2010;15:7115–24. https://doi.org/10.3390/molecules15107115.

[43] Annunziata G, Maisto M, Schisano C, Ciampaglia R, Narciso V, Tenore GC, et al. Resveratrol as a novel anti-herpes simplex virus nutraceutical agent: an overview. Viruses 2018;10. https://doi.org/10.3390/v10090473.

[44] Faith SA, Sweet TJ, Bailey E, Booth T, Docherty JJ. Resveratrol suppresses nuclear factor-B in herpes simplex virus infected cells. Antiviral Res 2006;72:242–51.

[45] Lin CJ, Lin HJ, Chen TH, Hsu YA, Liu CS, Hwang GY, et al. Polygonum cuspidatum and its active components inhibit replication of the influenza virus through Toll-like receptor 9-induced interferon beta expression. PLoS ONE 2015;10.

[46] Zang N, Xie X, Deng Y, Wu S, Wang L, Peng C, et al. Resveratrol-mediated gamma interferon reduction prevents airway inflammation and airway hyperresponsiveness in respiratory syncytial virus-infected immunocompromised mice. J Virol 2011;85:13061–8.

[47] Liu T, Zang N, Zhou N, Li W, Xie X, Deng Y, et al. Resveratrol Inhibits the TRIF-dependent pathway by upregulating sterile alpha and armadillo motif protein, contributing to anti-inflammatory effects after respiratory syncytial virus infection. J Virol 2014;88:4229–36.

[48] Mastromarino P, Capobianco D, Cannata F, Nardis C, Mattia E, De Leo A, et al. Resveratrol inhibits rhinovirus replication and expression of inflammatory mediators in nasal epithelia. Antiviral Res 2015;123:15–21. https://doi.org/10.1016/j.antiviral.2015.08.010.

[49] Cho JK, Curtis-Long MJ, Lee KH, Kim DW, Ryu HW, Yuk HJ, et al. Geranylated flavonoids displaying SARS-CoV papain-like protease inhibition from the fruits of Paulownia tomentosa. Bioorg Med Chem 2013;21:3051–7. https://doi.org/10.1016/j.bmc.2013.03.027.

[50] Kim HY, Eo EY, Park H, Kim YC, Park S, Shin HJ, et al. Medicinal herbal extracts of Sophorae radix, Acanthopanacis cortex, Sanguisorbae radix and Torilis fructus inhibit coronavirus replication in vitro. Antivir Ther 2010;15:697–709.

[51] Chen CN, Lin CPC, Huang KK, Chen WC, Hsieh HP, Liang PH, et al. Inhibition of SARS-CoV 3C-like protease activity by theaflavin-3,3′- digallate (TF3). Evidence-based Complement Altern Med 2005;2:209–15.

[52] Lin LT, Hsu WC, Lin CC. Antiviral natural products and herbal medicines. J Tradit Complement Med 2014;4:24–35. https://doi.org/10.4103/2225-4110.124335.

[53] Ryu YB, Jeong HJ, Kim JH, Kim YM, Park JY, Kim D, et al. Biflavonoids from Torreya nucifera displaying SARS-CoV 3CLpro inhibition. Bioorg Med Chem 2010;18:7940–7. https://doi.org/10.1016/j.bmc.2010.09.035.
[54] Cheng PW, Ng LT, Chiang LC, Lin CC. Antiviral effects of saikosaponins on human coronavirus 229E in vitro. Clin Exp Pharmacol Physiol 2006;33:612–6.
[55] Lin CW, Tsai FJ, Tsai CH, Lai CC, Wan L, Ho TY, et al. Anti-SARS coronavirus 3C-like protease effects of Isatis indigotica root and plant-derived phenolic compounds. Antiviral Res 2005;68:36–42.
[56] Lau KM, Lee KM, Koon CM, Cheung CSF, Lau CP, Ho HM, et al. Immunomodulatory and anti-SARS activities of Houttuynia cordata. J Ethnopharmacol 2008;118:79–85.
[57] Li SY, Chen C, Zhang HQ, Guo HY, Wang H, Wang L, et al. Identification of natural compounds with antiviral activities against SARS-associated coronavirus. Antiviral Res 2005;67:18–23.
[58] Sonja A. Rasmussen, MD, MS JCS. Dieckol, a SARS-CoV 3CLpro inhibitor, isolated from the edible brown algae Ecklonia cava. Bioorganic Med Chem J. 2020; January:19–21.
[59] Park HR, Yoon H, Kim MK, Lee SD, Chong Y. Synthesis and antiviral evaluation of 7-O-arylmethylquercetin derivatives against SARS-associated coronavirus (SCV) and hepatitis C virus (HCV). Arch Pharm Res 2012;35:77–85.
[60] Lee C, Lee JM, Lee NR, Kim DE, Jeong YJ, Chong Y. Investigation of the pharmacophore space of Severe Acute Respiratory Syndrome coronavirus (SARS-CoV) NTPase/helicase by dihydroxychromone derivatives. Bioorg Med Chem Lett 2009;19:4538–41. https://doi.org/10.1016/j.bmcl.2009.07.009.
[61] Lee C, Lee JM, Lee NR, Jin BS, Jang KJ, Kim DE, et al. Aryl diketoacids (ADK) selectively inhibit duplex DNA-unwinding activity of SARS coronavirus NTPase/helicase. Bioorg Med Chem Lett 2009;19:1636–8. https://doi.org/10.1016/j.bmcl.2009.02.010.
[62] Park JY, Yuk HJ, Ryu HW, Lim SH, Kim KS, Park KH, et al. Evaluation of polyphenols from Broussonetia papyrifera as coronavirus protease inhibitors. J Enzyme Inhib Med Chem 2017;32:504–12.
[63] Ho TY, Wu SL, Chen JC, Li CC, Hsiang CY. Emodin blocks the SARS coronavirus spike protein and angiotensin-converting enzyme 2 interaction. Antiviral Res 2007;74:92–101.
[64] Yi L, Li Z, Yuan K, Qu X, Chen J, Wang G, et al. Small molecules blocking the entry of severe acute respiratory syndrome coronavirus into host cells. J Virol 2004;78:11334–9.
[65] Mahbub AA, Le Maitre CL, Haywood-small S, Cross NA, Jordan-mahy N. Polyphenols enhance the activity of alkylating agents in leukaemia cell lines. Oncotarget 2019;10:4570–86.
[66] Ren KW, Li YH, Wu G, Ren JZ, Bin LuH, Li ZM, et al. Quercetin nanoparticles display antitumor activity via proliferation inhibition and apoptosis induction in liver cancer cells. Int J Oncol 2017;50:1299–311.
[67] Turumtay H, Midilli A, Turumtay EA, Demir A, Selvi EK, Budak EE, et al. Gram (−) microorganisms DNA polymerase inhibition, antibacterial and chemical properties of fruit and leaf extracts of Sorbus acuparia and Sorbus caucasica var. yaltirikii. Biomed Chromatogr 2017;31. e3901.
[68] Nosrati M, Shakeran Z, Shakeran Z. Frangulosid as a novel hepatitis B virus DNA polymerase inhibitor: a virtual screening study. In Silico Pharmacol 2018;6:10.
[69] Wu Y, Hsieh T, Wu JM, Wang X, Christopher JS, Pham AH, et al. Elucidating the inhibitory effect of resveratrol and its structural analogs on selected nucleotide- related enzymes. Biomolecules 2020;10:1223. https://doi.org/10.3390/biom10091223.
[70] Lepak A, Gutmann A, Kulmer ST, Nidetzky B. Creating a water-soluble resveratrol-based antioxidant by site-selective enzymatic glucosylation. ChemBioChem 2015;16:1870–4.
[71] Hollman PCH, Bijsman MNCP, Van Gameren Y, Cnossen EPJ, De Vries JHM, Katan MB. The sugar moiety is a major determinant of the absorption of dietary flavonoid glycosides in man. Free Radic Res 1999;31:569–73. https://doi.org/10.1080/10715769900301141.
[72] Gupta S, Singh AK, Kushwaha PP, Prajapati KS, Shuaib M, Senapati S, et al. Identification of potential natural inhibitors of SARS-CoV2 main protease by molecular docking and simulation studies. J Biomol Struct Dyn 2020. https://doi.org/10.1080/07391102.2020.1776157.
[73] Ratia K, Pegan S, Takayama J, Sleeman K, Coughlin M, Baliji S, et al. A noncovalent class of papain-like protease/deubiquitinase inhibitors blocks SARS virus replication. Proc Natl Acad Sci USA 2008;105:16119–24. https://doi.org/10.1073/pnas.0805240105.
[74] Mhatre Susmit, Gurav Nitisha, Shah Mansi, Patravale Vandana. Entry-inhibitory role of catechins against SARS-CoV-2 and its UK variant. Comput Biol Med 2021;135:104560. https://doi.org/10.1016/j.compbiomed.2021.104560.
[75] Rut Wioletta, Lv Zongyang, Zmudzinski Mikolaj, Patchett Stephanie, Nayak Digant, et al. Activity profiling and crystal structures of inhibitorbound SARS-CoV-2 papain-like protease: A frameworkfor anti–COVID-19 drug design. Sci Adv 2020;6. https://doi.org/10.1126/sciadv.abd4596.